

A Low Cost Picoseconds Precision Timing and Synchronization Over A Hundred Kilometer

Alice Renaux*, Ronic Chiche*, Aurélien Martens*, Antoine Back*, Paul-Eric Pottier†, and Daniel Charlet*

* Laboratoire de Physique des 2 Infinis Irène Joliot-Curie (IJCLab), Université Paris-Saclay, CNRS/IN2P3
Orsay, France

† Laboratoire Temps Espace (LNE-OP), Observatoire de Paris, Université PSL, Sorbonne Université, Université
de Lille, LNE, CNRS
Paris, France

Email: aurelien.martens@ijclab.in2p3.fr

Abstract—Large-scale systems, such as very large accelerators used for fundamental research, require the implementation of precise timing and synchronization systems over distances of several tens of kilometers. A very high precision has been demonstrated by the use of costly and complex clock distribution systems. However, many devices, such as accelerator diagnostics or large-scale detectors, only require picosecond precision. An approach exploiting the CERN White Rabbit protocol, deployed and enhanced on an electronic system capable of generating arbitrary frequencies with Hertz precision, is proposed here. Results of performance tests for the synchronization of a laser system, typically employed as a diagnostic for electron/positron beam polarimetry in accelerators, are provided in this Paper. We demonstrate that without implementing corrections for environmental changes, as temperature drifts, the system can synchronize a pulsed laser with picoseconds precision over a hundred kilometers, exhibiting drifts of a few picoseconds. This work paves the way for a low-cost implementation of picosecond synchronization of accelerator components and large-scale detectors.

Index Terms—Time synchronization, Frequency stability, Phase noise, Measurement uncertainty, White Rabbit (WR), Precision Time Protocol (PTP), Optical fiber links, Synchronous Ethernet (SyncE), Distributed timing systems, Metrology, Particle physics experiments, Particle accelerators, Laser feedback.

I. INTRODUCTION

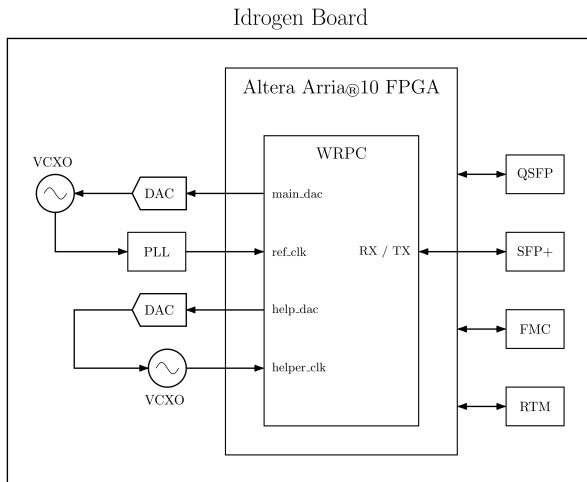
LARGE accelerators, as colliders, generally employed for fundamental research in particle physics, are of a few tens of kilometers in circumference, see for instance the Large Hadron Collider (LHC) at CERN [1] and to a lesser extent the SuperKEKB collider at KEK in Japan [2]. Future projects are of even larger scale, as considered for a linear collider [3], [4], or for circular colliders [5], [6], where the ring circumference is expected to be larger than 90 kilometers. These accelerators require that diagnostics be properly synchronized. Accurate bunch identification, as required for the polarimetry of circulating beams, further necessitates precise timing [6], [7]. Very high stability has been achieved in large-scale accelerators for high-brilliance radiation sources at the European X-FEL [8]–[12]. The distribution of time standards over large scales has also been demonstrated in the past few decades [13]–[15]. These costly all-optical systems or electro-optical systems are also implemented in existing colliders, where the most

stringent requirement is imposed by the use of selective accelerating cavities [16], [17]. A White-Rabbit protocol-based RF distribution is being considered as a reference for the high-luminosity upgrade of the LHC [18], [19]. Timing of large detectors with the accelerator also imposes some constraints on the stability of these links, but at a moderate level of picosecond precision [20]–[22]. The use of bunch-per-bunch beam position monitor also allows for the diagnosis with precision of dramatic events occurring in these large-scale colliders, detrimental to their performances, and where a picosecond timing system, easily integrable in an existing facility, is of interest [23]. Furthermore, the use of polarized beams in future colliders and upgrades of existing colliders necessitates the implementation of laser-based diagnostics, such as Compton polarimeters [3]–[7], [24], [25]. The use of modern laser technology, exploiting passively mode-locked laser oscillators with picosecond pulse durations, is considered for these projects. As a consequence, picosecond timing and synchronization of the laser with the few-picosecond-duration bunches of the accelerator is needed. The accelerator clock must be distributed over the scale of the accelerator, of several tens of kilometers for the largest. Existing systems employ the distribution of the absolute accelerator radio-frequency reference, the Master Oscillator (MO), clock through optical fibers, whose drifts are compensated for to achieve a precision of typically a hundred femtoseconds in the clock transfer, with latencies related to the fiber length [16], [26]. These systems are costly and also slightly overspecified for synchronizing the above-mentioned diagnostics. They are, moreover, difficult to implement, as they require some significant and expensive integration adjustments. The work described in this paper aims to demonstrate the proof of concept for a low-cost solution that achieves picosecond precision synchronization of a diagnostic integrated into an accelerator with minimal integration requirements. To that end, we utilize an electronics system developed at IJCLab that leverages the White Rabbit protocol [32], [33]. It is shortly described in section II. This system is implemented in a laboratory room to synchronize a commercial laser system, representative of those used for accelerator diagnostics, but also for photocathode systems. The

arXiv:2602.20622v1 [physics.acc-ph] 24 Feb 2026

test setup is described in Section III. Obtained results and prospects for improvements are further discussed in section IV, before drawing conclusions.

II. THE IDROGEN SYSTEM



(a) Sketch of Idrogen board WR integration.



(b) Photograph of assembled Idrogen board. The outer dimensions are 15×10 cm.

Fig. 1. Views of the Idrogen board.

Idrogen board is a μ TCA board based on an Altera Arria@10 FPGA. This FPGA was chosen for its performance/price ratio. The main hardware elements of the Idrogen board are illustrated in Fig.1. At the heart of the Idrogen lies a high-speed FPGA that orchestrates all board functionalities, serving as the central controller for communication, timing, and signal processing tasks. This board has been designed to comply with the WR protocol [32], [33]. Figure 1a is a schematic representation of WR implementation on Idrogen board.

A critical feature of the design is an ultra-low-noise clock tree, built around the Texas Instruments LMK04828 jitter cleaner, which offers an outstanding root-mean-square jitter of 91 fs (integrated over 100 Hz to 20 MHz). The LMK04828

features an integrated VCO operating near 3 GHz and provides JESD204B-compliant clocking capabilities. Additionally, up to seven SYSREF signals are available to support high-precision acquisition synchronization for daughter cards or subsystems.

The LMK04828 is phase and frequency locked by a 100 MHz ultra-low-phase-noise oscillator (RAKON 1490U), featuring a phase noise of -116 dBc/Hz at 10 Hz offset — a specification we have carefully verified experimentally. The clock cleaner further accepts two external clock inputs, covering a frequency range from 10 MHz to 500 MHz, with a tunable loop bandwidth between 1 kHz and 100 kHz. This flexibility enables Idrogen to operate as a Grandmaster (GM) with exceptionally low additive phase noise when locked to an external reference.

The WR core is implemented within the FPGA and operated in slave mode. The FPGA dynamically controls a low-noise 16-bit 20 kS/s digital-to-analog converter (DAC) to apply voltage tuning to the local 100 MHz oscillator, correcting frequency offsets according to the WR core (wrc). We implemented WRC version 5 in the FPGA.

In addition, the FPGA manages the generation of a helper clock used within the Digital Dual Mixer Time Difference (DDMTD) architecture [34]. To improve phase sensitivity and simplify the FPGA design, the DDMTD is operated at 125 MHz, twice the carrier frequency compared to the WR original implementation.

The Idrogen board features one SFP+ port and one QSFP port. The SFP+ port is used to establish the 1Gb/s WR link. In parallel, the QSFP interface provides a data output capability of 40Gb/s, a critical feature for use cases requiring high-speed synchronous sampling, such as accelerator diagnostics, to name only one.

Particular attention has been paid to provide high-stability performance. In parallel, a complete firmware and software ecosystem was developed to control and monitor the Idrogen board, including WR core parameters, using IPBus or PCIe protocols. These tools provide access to the WR command-line interface (CLI) and, therefore, to the graphical user interface (GUI) for more intuitive supervision. It provides access to key parameters of the WR core (WRC), especially the software-based phase-locked loop (SPLL), where the proportional and integral gains can be dynamically adjusted. This flexibility is particularly advantageous for optimizing phase noise performance and adapting to different fiber link lengths.

The μ TCA implementation of Idrogen additionally provides full remote management and supervision capabilities, consistent with standard μ TCA platform management frameworks. Furthermore, the generated clock signals can be broadcast over dedicated clock distribution channels reserved within the μ TCA backplane, enabling precise timing dissemination across the crate.

The Idrogen board has been designed to be a generic and modular system. A FMC slot enables the extension of board capabilities, for example, with an ADC FMC board, allowing it to be used as a high data rate acquisition system synchronized by WR and compliant with JESD204B. Additional functionalities can be integrated through dedicated RTM (Rear Transition Module) extension boards. The implementation of

the White Rabbit protocol within the FPGA enables precise time-stamping and time-tagging of all events acquired by the extension, as well as of any signals or data streams processed internally by the FPGA.

III. THE TEST SETUP

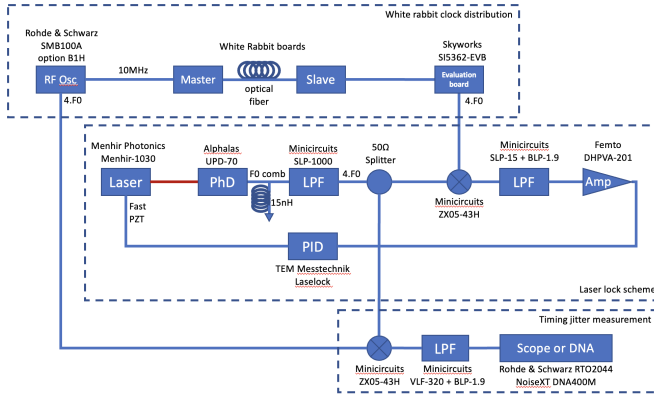


Fig. 2. Diagram of the implemented test setup, see text for details.

This electronic system is installed in a roughly thermally stabilized room, typically used for laser experiments, where the temperature is expected to vary by a couple of degrees at most. The intention is to validate the performance of clock transfer and locking of a MENHIR-1030 from MENHIR-PHOTONICS AG. This laser system is representative of passively mode-locked laser systems designed for use in Compton polarimeters in accelerators. It is equipped with two piezoelectronic transducers (PZTs) for the tuning of the repetition rate around its nominal value of $F_0 = 216.661555 \text{ MHz}$. The diagram corresponding to the implemented setup is given in Fig.2. To validate the performance of the synchronization system, the master Idrogen board (MIB) is disciplined by a 10 MHz reference from a Rhode & Schwarz SMB100A microwave signal generator equipped with an OCXO B1H. Another Idrogen board (SIB), locked through a White Rabbit link on the MIB, generates a 250 MHz LVDS signal that is provided to a SIS362-EVB-A from SkyWorks (SIC). The fiber link between MIB and SIB can be configured to be either 10 m, 5 km, 50 km or 100 km long. The SIS362 chip embedded on the SIC allows arbitrary frequency generation, with Hertz precision, synchronous to the SIB output. The SIC is configured with two outputs that deliver clocks at the fourth harmonic, $4F_0$, of the laser frequency and one at F_0 . One of the $4F_0$ outputs is passively mixed (ZX05-43H from Minicircuits) with the microwave signal obtained by sending the laser light to a UPD-70 photo-diode from Alphasalas GmbH, amplified, and filtered. The choice of filters is not optimal, but it reflects the limited component selection available at the time of measurement. A quick check of the measured spectrum with a spectrum analyzer shows that the $4F_0$ is the largest contribution, with extinction of other harmonics by at least 20 dB. The mixed output is filtered and used as an error signal to seed a commercial PID corrector. The Laselock[®] from TEM Messtechnik GmbH is configured to drive both PZTs

of the laser. A split of the amplified output of the laser photodiode is used for diagnostics, such as long-term phase drift and short-term phase noise power spectral density measurement.

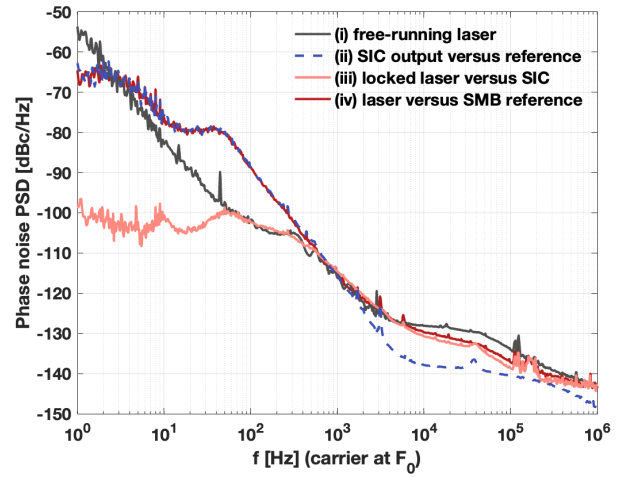


Fig. 3. Power spectral density of phase noise for the (i) free running laser; (ii) the SIC output with respect to the reference; (iii) the technical noise of the laser loop on the SIC output; (iv) the laser output with respect to the reference.

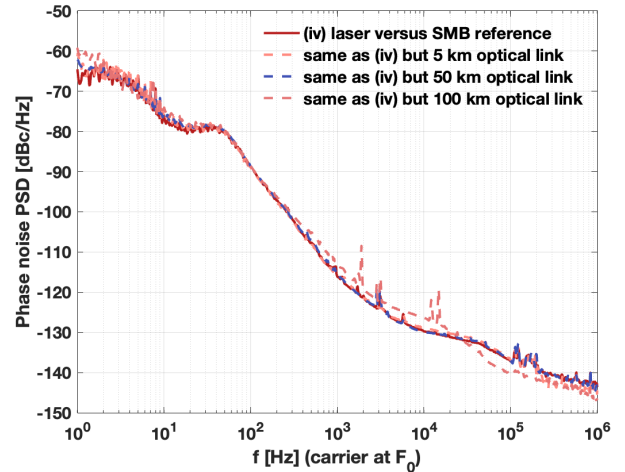


Fig. 4. Power spectral density of phase noise for the (iv) the laser output with respect to the reference with 10 m, 5 km, 50 km and 100 km fibre links. A difference can be spotted with the 100 km where the noise is slightly larger above 300 Hz. Preliminary investigations suggest that this might be due to a change of the measurement setup where amplifiers have been added after the 50 Ohm splitter.

The power spectral density of phase noise is measured with a NoiseXT DNA-400M Digital Noise Analyzer (DNA). Its bandwidth is limited to 400 MHz, so only microwave signals at F_0 are measured. Several measurements are performed: (i) the free-running laser output without the amplifier after the photodiode; (ii) the output of the SIC at F_0 ; (iii) the output of the laser, locked on the SIC, measured with respect to the SIC reference at F_0 ; (iv) the output of the laser, locked on the SIC, measured with respect to the SMB reference at F_0 . The results are shown in Fig. 3. The computed integrated phase

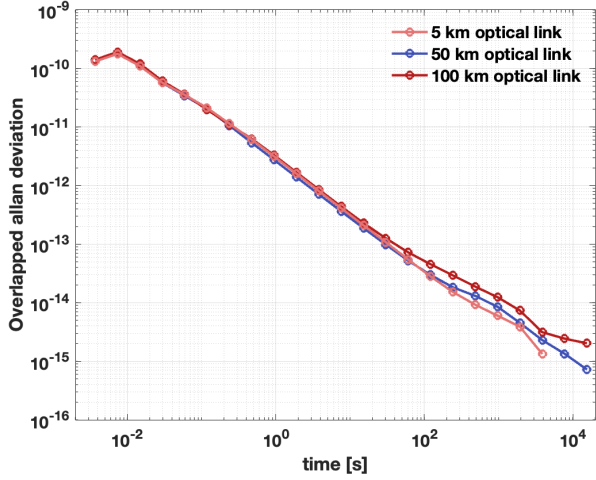


Fig. 5. Measurement of the overlapped allan deviation of the laser locked on the SIC with respect to the SMB reference, for various fibre length.

noise is 1.4 ps RMS over the measurement range. We note the excellent consistency of the measurement of the locked laser onto the SIC, the SIC output, and the added technical noise by the laser/SIC loop. We have checked that the phase noise of the free running laser measured after the splitter follows the curve (iii) above 50 Hz. It results in an apparent degradation of the exquisite laser phase noise due to the measurement chain rather than a genuine degradation of the laser phase noise. A measurement of the laser phase noise in the optical domain is necessary to conclude on this aspect, which is out of the scope of this proof of concept paper. These results state the current performance of the system. It has been reproduced with an E5052A SSA from Agilent. These results were obtained with a 10 m long fibre link between the MIB and SIC boards. We observe no modification of the power spectral density of residual phase noise when replacing it with a 5 km and 50 km fibre link because the deviation frequency range is limited to 1 Hz at low frequency. The use of a 100 km fibre link however exhibits two differences. At low deviation frequencies, around 1 Hz, the system seems slightly less stable. It might be due to the addition of an optical amplifier in the middle point of the fibre to allow enough signal to reach the transceivers. Above 300 Hz a modification of the phase noise spectral density is observed. This confirms the assumption that this part of the spectrum is rather dominated by technical noises, as amplifiers were added on both outputs of the 50 ohm splitter. The result is shown in Fig. 4. The modified Allan deviation is measured to be approximately 3.1×10^{-12} at 1 s with a regular τ^{-1} decay for the laser synchronized to the SIC, measured relative to the SMB reference, as shown in Fig.5. A departure of the allan deviation on timescales of about 10 s is observed for the 100 km fibre link (including the fibre amplifier), compared to other measurements. This effect is left for further investigations.

To further complement these measurements, a phase detection is realized between the amplified RF signal from the photodiode and the SIC 866.66 MHz output using a passive mixer and filter. It has been realized for the various fibre

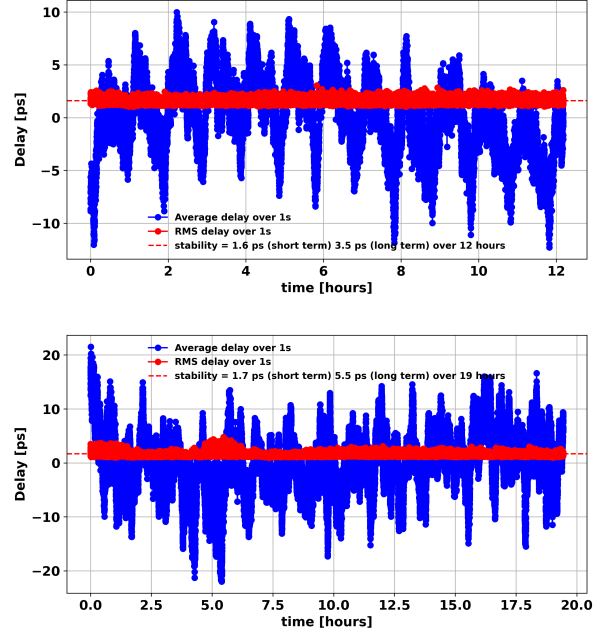


Fig. 6. The measurements over 12 (19) hours of the mean and RMS delay measured over one second (forty million samples) between the laser locked on the SIC and the SMB reference, virtually located 50 (top) and 100 (bottom) kilometers away from the laser.

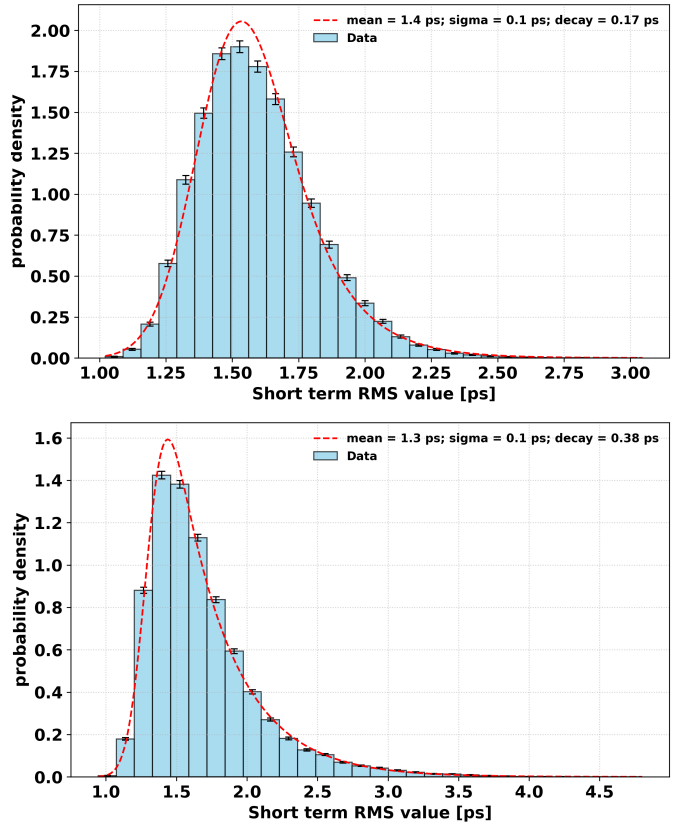


Fig. 7. Histogram of the measured RMS delay showing a near Gaussian behavior with a mean of 1.6 ps and width of 0.2 ps and 1.7 ps and width of 0.4 ps, for 50 km (top) and 100 km (bottom), respectively. The dashed red curve corresponds to a Gaussian fit to the data.

lengths. Results with 50 km are presented in the following. The phase is acquired with an oscilloscope. While opening the laser/SIC locking loop, a clean sine signal is observed with a large amplitude of about 700 mV. We then close the loop and measure the calibrated phase difference. Waveforms of one second duration are acquired and analyzed in real-time by the apparatus to extract the standard deviation and the average phase. It is tracked for several hours and shown on Fig. 6. We observe excellent reproducibility of the standard deviation of the phase, which is perfectly consistent with the measured phase noise of the DNA, as shown in Fig. 7. The average phase over a second exhibits variations with a period of approximately one hour, likely related to the cycling of the room's air conditioning. These likely explain the observed variations. Note that during these measurements, the boards were not encapsulated in housing with thermal control, nor in μ TCA crates. The results with the 100 km were found to exhibit long term stability worse by a factor larger than 1.5, at 5.5 ps RMS. The distribution of the measured RMS delays gets more peaky at 1.4 ps with a longer tail at larger RMS values, suggesting a less stable operation. An exponentially convoluted Gaussian distribution [35] is found to fit the data well and is motivated by the observation that thermal variations induce a shift in the delay with some finite relaxation time. It allows for representing the presence of a positive definite additive delay. The obtained mean of the Gaussian is consistent with the RMS jitter computed from the phase noise PSD, as expected. The time over which the laser could be kept locked was found very different from one day to another, likely due to different environmental conditions. Further investigations, with encapsulated or racked boards, are kept out of the scope of this proof of concept paper, and will allow to conclude on this aspect.

IV. DISCUSSION

The obtained results demonstrate that picoseconds-level synchronization has been achieved for two microwave clocks, virtually separated by a hundred kilometers of regular fiber link, using a low-cost electronic system that exploits the White Rabbit protocol. Consistency is achieved between the measurements of the power spectral density of phase noise and phase difference with respect to the reference clock at 866 MHz. The apparent degradation of laser phase noise when in the measurement chain, above 50 Hz, might be solved in the future for some dedicated applications that require exquisite phase noise [27], [28]. The test was conducted with boards simply placed on a table, and neither encapsulated in housing nor integrated into racks, as would be necessary for integration in an accelerator. The observed drift of the relative phase over hours of operation is likely due to environmental variations. These issues will likely be mitigated with proper housing and venting of the boards or incorporation into μ TCA crates, which remains to be tested but is outside the scope of this proof-of-principle work. Preliminary investigations suggest that this effect is mainly related to the SI5362-EVB. Implementation of corrections for known temperature changes, exploiting probes embedded on the *ldrogen* boards, is planned. The work also

demonstrates that the lock of the laser was preserved for 16 hours without loss, a duration limited here by the allocated time for the experiments and the availability of the hardware. Longer tests will be performed at a later stage. The development of an FMC with the SI5362 chip is also underway to fully leverage the modularity of the *ldrogen* system, resulting in a compact, low-cost, and arbitrary frequency generator with sub-picosecond timing that is easily integrated into an accelerator environment. The hope is that these developments will significantly help understanding and possibly improving the long term stability of the system.

V. CONCLUSION

The results presented in this paper demonstrate that a frequency generation method exploiting the White Rabbit protocol, embedded and enhanced in the *ldrogen* board, enables achieving picosecond-level precision over a 1-s window with drifts of up to 20 ps peak-to-peak observed over 16 hours. These are planned to be mitigated by a proper encapsulation of boards and further temperature corrections. The present result already leverage the possibility to implement this system in accelerator for further experimental performance validation, as synchronization of photocathode laser systems for beam generation [17], Compton polarimeters [7] and interaction with beams [27], [28], and acquisition of bunch-per-bunch beam profile monitors, exploiting the capability of *ldrogen* to embed a 1 GHz FMC ADC [23]. It further paves the way for the use of this technology in low-cost picosecond arbitrary frequency generation in large-scale facilities, where scalability is a crucial aspect [29]. Large detectors located on large colliders also represent an area of application of the concept evaluated here [30], with possible implications in cosmic ray detection and medical physics [31].

ACKNOWLEDGMENTS

The authors thank K. Popov from KEK ATF, iCASA, and C. Joly from IJCLab for fruitful discussions. Part of the instrumentation was funded by the "Investissements d'Avenir" programme launched by the French Government and implemented by the Agence Nationale de la Recherche (ANR) under reference ANR-21-ESRE-0029 (ESR/Equipex+T-REFIMEVE). This research has been partly funded by Agence Nationale de la Recherche (ANR) by the project ANR-25-CE31-7501-01.

REFERENCES

- [1] L. Evans and P. Bryant, "LHC Machine," *Journal of Instrumentation*, vol. 3, pp. S08001, 2008.
- [2] N. Toge (ed.), "KEK B-factory design report," *KEK note*, 95-7, 1995.
- [3] T.K. Charles and others, "The Compact Linear Collider (CLIC) 2018 Summary report," *CERN Yellow reports*, CERN-2018-005-M, 2018.
- [4] C. Adolphsen and others, "The International Linear Collider Technical Design Report - Volume 3.II: Accelerator Baseline Design," 2013, <https://arxiv.org/abs/1306.6328>.
- [5] J. Gao, "CEPC Technical Design Report: Accelerator," *Radiat Detect Technol Methods* 8, 1–1105 (2024).
- [6] M. Benedikt and others, "Future Circular Collider Feasibility Study Report Volume 2: Accelerators, technical infrastructure and safety," *CERN reports*, 2025, <https://arxiv.org/abs/2505.00274>.

- [7] D. Charlet and others, "Conceptual study of a Compton polarimeter for the upgrade of the SuperKEKB collider with a polarized electron beam," *Journal of Instrumentation*, vol. 10, pp P10014, 2023.
- [8] J. Frisch, D. Bernstein, D. Brown and E. Cisneros, "A high stability, low noise RF distribution system," in *Proceedings of the 2001 Particle Accelerator Conference, Chicago, IL, USA, 2001*, pp. 816-818 vol.2, doi: 10.1109/PAC.2001.986485.
- [9] S. Schulz, A.-L. Calendron, M.K. Czwalinna, M. Felber, A. Grünhagen, T. Kozak, N. Kschuev, T. Lamb, B. Lautenschlager, H. Schlarb, M. Schütte, D. Schwickert, F. Zummack, "Latest achievements in femtosecond synchronization of large scale facilities," in *Proceedings of IPAC 2025*, doi:10.18429/JACOW-IPAC2025-FRZD1.
- [10] Schulz, S., Grguraš, I., Behrens, C. et al., "Femtosecond all-optical synchronization of an X-ray free-electron laser", *Nat. Commun.* 6, 5938 (2015).
- [11] M. Xin, K. Şafak, and F. Kärtner, "Ultra-precise timing and synchronization for large-scale scientific instruments," *Optica* 5, 1564-1578 (2018).
- [12] J. Tratnik, L. Pavlovic, B. Batagelj, L. Naglic, T. Korosec and M. Vidmar, "Electro-optical synchronization system with femtosecond precision," in *2010 Conference on Optical Fiber Communication (OFC/NFOEC), collocated National Fiber Optic Engineers Conference, San Diego, CA, USA, 2010*, pp. 1-3, doi:10.1364/OFC.2010.OThH4.
- [13] M. Fujieda, M. Kumagai, T. Gotoh and M. Hosokawa, "Ultrastable Frequency Dissemination via Optical Fiber at NICT," in *IEEE Transactions on Instrumentation and Measurement*, vol. 58, no. 4, pp. 1223-1228, April 2009.
- [14] M. Lessing, H. S. Margolis, C. T. A. Brown, et G. Marra, "Frequency comb-based time transfer over a 159 km long installed fiber network", *Applied Physics Letters*, vol. 110, p. 221101, 2017
- [15] O. Lopez et al., "Simultaneous remote transfer of accurate timing and optical frequency over a public fiber network", *Applied Physics B*, vol. 110, pp. 3-6, 2013
- [16] T. Kobayashi et al., "LLRF controls in SuperKEKB Phase-1 commissioning", 2018, <https://arxiv.org/abs/1803.09037>.
- [17] Popov, K. and Aryshev, A. and Terunuma, N., "KEK ATF Linac, Damping Ring accelerating field and RF-Gun laser system phase&litude stability study", *Journal of Physics: Conference Series*, vol. 3094, pp. 012044, 2025.
- [18] T. Wlostowski et al., "White Rabbit and MTCA.4 Use in the LLRF Upgrade for CERN's SPS", in *Proc. ICALEPCS'21, Shanghai, China, Mar. 2022*, pp. 847-852, doi:10.18429/JACoW-ICALEPCS2021-THBR02
- [19] P. Hazell et al., "Phase stability compliancy testing of a White Rabbit based solution for the LHC RF and Timing Distribution Backbone upgrade", *Journal of Instrumentation*, vol. 19, p. C12019, 2024.
- [20] J. Varela, "Timing and synchronization in the LHC experiments", *CERN report*, CMS-CR-2000-012, doi: 10.5170/CERN-2000-010.77.
- [21] Cavallari, F., "High performance timing detectors for high energy physics experiments and new developments for the high luminosity LHC", *Journal of Instrumentation*, vol. 15, p C03041, 2020. doi: 10.1088/1748-0221/15/03/C03041
- [22] T. Masuda, "Timing signal distribution for synchrotron radiation experiments using RF over White Rabbit," in *17th Int. Conf. on Acc. and Large Exp. Physics Control Systems, WEPHA096*, page 1316, doi:10.18429/JACoW-ICALEPCS2019-WEPHA096.
- [23] Riku Nomaru and Gaku Mitsuka and Larry Ruckman, "Measurement of Sudden Beam Loss Events Using Bunch-by-Bunch BPMs at SuperKEKB", 2025, <https://arxiv.org/abs/2507.13617>.
- [24] Willeke, Ferdinand, and Beebe-Wang, J., "Electron Ion Collider Conceptual Design Report 2021," 2021, <https://doi.org/10.2172/1765663>.
- [25] Z. Duan et al., "A preliminary design of a Compton polarimeter at BEPCII", in *Proc. IBIC2024, Beijing, Sep. 2024*, pp. 645-648, doi:10.18429/JACoW-IBIC2024-THP72
- [26] T. Akiyama, H. Matsuzawa, E. Haraguchi, T. Ando and Y. Hirano, "Phase stabilized RF reference signal dissemination over optical fiber employing instantaneous frequency control by VCO," in *IEEE/MTT-S International Microwave Symposium Digest, Montreal, QC, Canada, 2012*, pp. 1-3, doi:10.1109/MWSYM.2012.6258332.
- [27] M. Alkadai et al., "Commissioning of ThomX Compton source subsystems and demonstration of 10^{10} x-rays/s," *Phys. Rev. Accel. Beams*, vol. 28, pp. 023401, 2025, doi:10.1103/PhysRevAccelBeams.28.023401.
- [28] A. Martens et al., "Design of the optical system for the gamma factory proof of principle experiment at the CERN Super Proton Synchrotron," *Phys. Rev. Accel. Beams*, vol. 25, pp. 101601, 2025, doi:10.1103/PhysRevAccelBeams.25.101601.
- [29] F. Torres-González, J. Díaz, E. Marín-López and R. Rodríguez-Gómez, "Scalability analysis of the white-rabbit technology for cascade-chain networks," in *IEEE International Symposium on Precision Clock Synchronization for Measurement, Control, and Communication (ISPCS), Stockholm, Sweden, 2016*, doi: 10.1109/ISPCS.2016.7579515.
- [30] J Va'vra, "Precision Timing Detectors in Particle Physics: Progress and Challenges in Picosecond Resolution Technologies," *Current Research Progress in Physical Science*, Vol. 2, pp.108-141, 2024.
- [31] C. Royon, F. Gautier, "Fast timing detectors with applications in cosmic ray physics and medical science", *Nuclear Instruments and Methods in Physics Research Section A: Accelerators, Spectrometers, Detectors and Associated Equipment*, vol. 1058, pp. 168886, 2024.
- [32] J. Serrano, M. Cattin, E. Gousiou, E. van der Bij, T. Wlostowski, G. Daniluk, M. Lipinski, "The White Rabbit project", *2nd International Beam Instrumentation Conference, Oxford, UK, 16 - 19 Sep 2013*, pp.THBL2.
- [33] M. Lipiński, T. Wlostowski, J. Serrano and P. Alvarez, "White rabbit: a PTP application for robust sub-nanosecond synchronization," *2011 IEEE International Symposium on Precision Clock Synchronization for Measurement, Control and Communication, Munich, Germany, 2011*, pp. 25-30, doi: 10.1109/ISPCS.2011.6070148.
- [34] P. Moreira, P. Alvarez, J. Serrano and I. Darwazeh, "Sub-nanosecond digital phase shifter for clock synchronization applications," *2012 IEEE International Frequency Control Symposium Proceedings, Baltimore, MD, USA, 2012*, pp. 1-6, doi: 10.1109/FCS.2012.6243715.
- [35] E. Grushka, "Characterization of exponentially modified Gaussian peaks in chromatography", *Analytical Chemistry*, Vol. 44, pp. 1733-1738, 1972.